WILEY ONLINE LIBRARY
Early View publication on wileyonlinelibrary.com
(issue and page numbers not yet assigned;
citable using Digital Object Identifier – **DOI**)

Phys. Status Solidi C, 1–4 (2012) / **DOI** 10.1002/pssc.201200130

physica status solidi c
www.pss-c.com
current topics in solid state physics

Optical properties and carrier transport in c-Si/conductive PEDOT:PSS(GO) composite heterojunctions

Zeguo Tang, Qiming Liu, Ishwor Khatri, Ryo Ishikawa, Keiji Ueno, and Hajime Shirai*

Graduate School of Science and Engineering, Saitama University, Saitama 338-8570, Japan

Received 1 May 2012, revised 11 June 2012, accepted 11 June 2012
Published online 8 August 2012

Keywords c-Si/organic junction, solar cells, carrier transport, PEDOT:PSS, graphene oxide

* Corresponding author: e-mail shirai@fms.saitama-u.ac.jp

We investigated the crystalline silicon (c-Si)/conductive poly(ethylene dioxythiophene):poly(styrene sulfonate) (PEDOT:PSS):graphene oxide (GO) composite heterojunction devices with optical characterization and carrier transport measurement techniques. The optical transmittance in the UV region also decreased markedly for the films with GO content above 20 wt%, whereas it increased markedly in the visible-infrared regions. The solar cell devices consisting of spin-coated PEDOT:PSS(GO) composite on n-type c-Si(100) wafer exhibited a maximum efficiency of 10.3%, a short-circuit current J_{sc} of 28.9 mA/cm^2, a open-circuit voltage V_{oc} of 0.548 V, and a fill factor *FF* of 0.675 at a GO content of 12.5 wt%. The ideality factor deduced from current density-voltage (*J*-V) plots in the dark increased with GO content from 1.12 for pristine PEDOT:PSS to 2.91. Temperature-dependent dark *J*-V measurements suggest that the carrier transport in the devices is controlled by diffusion and recombination in the space-charge region for the devices. The role of the GO addition into conductive PEDOT:PSS is demonstrated for the c-Si(100)/-PEDOT:PSS(GO) composite junction solar cells in terms of the optical and carrier transport properties.

1 Introduction Solar cells based on crystalline silicon (c-Si) p-n junction offer high power-conversion efficiency η of 24-25%, but high temperature process of above 1000˚C is required. The c-Si based heterojunction solar cells with an intrinsic hydrogenated amorphous silicon (a-Si:H) thin layer (HIT) also offer high η values of 22-23% due to higher open-circuit voltage V_{oc} values and a better surface passivation [1, 2]. Here, low-pressure plasma CVD sputtering are used for the fabrication of a-Si:H and indium-tin-oxide (ITO) layers. The alternate approach using organic solar cells (OSCs) have been extensively studied due to their potential as a renewable, alternative source of electricity and their preference in low cost, light weight, mechanical flexibility, and easy processing conditions such as spin-coating [3]. For the hole collection in common solar cells, spin-coated poly(ethylene dioxythiophene):poly(styrene sulfonate) (PEDOT:PSS) is often used to modify the ITO electrode in view of the superior injection/collection properties of the PEDOT:PSS/active layer compared to those of the ITO/active layer interface [4]. But the efficiency of OSCs is not efficient. Recently, efficient c-Si/PEDOT:PSS junction solar cells have been reported [5]. However, little studies on the optical properties and carrier transport in the c-Si/PEDOT:PSS junctions have been performed.

In this paper, we demonstrate the optical and carrier transport properties of the c-Si/PEDOT:PSS(GO) composite heterojunction solar cell devices by optical transmittance, current density-voltage-temperature (*J*-V-T) characteristics, and spectra response measurements.

2 Experimental details One-side-polished n-type CZ silicon wafers with an average resistivity of 3-5 Ω·cm (N_D~10^{15} cm^{-3}) were used as a substrate. The c-Si wafer was cleaned by (1) RCA1 cleaning at solution of NH_4OH: H_2O_2 = 5:1 heated at 80 °C for 10 minutes, (2) HF dipping (5%, 1 min), (3) RCA2 cleaning at solution of HCl: H_2O_2 = 5:1 heated at 80 °C for 10 minutes, (4) HF dipping (5%, 1 min), deionized water cleaning for 10 minutes. A functionalized GO used in this study was prepared by a modified

Hummers method, a chemical oxidation method [6, 7]. The average size of GO flake sheets was 1-5 μm. GO is highly soluble in an aqueous solution, and therefore, it is well dispersed in the PEDOT:PSS (Clevios PH1000). The schematic of the photovoltaic devices used in this study is shown in Fig. 1, which has a structure of Ag grid/conductive PEDOT:PSS(GO)/c-Si/Al. The PEDOT:PSS(GO) composite diluted in methanol was spin-coated on c-Si(100) wafer. For comparison, photovoltaic devices based on a buffer layer of c-Si/pristine PEDOT:PSS junction having a similar device structure were also prepared. After spin coating of the pristine PEDOT:PSS(GO) films, thermal annealing at 140 °C for 30 min was conducted to remove the residual solvent. The thickness of PEDOT:PSS(GO) composite was 100 nm. The active area of the device, as defined by the top electrode, was 5×5 mm^2. The *J*-V characteristics were measured in the dark and under light illumination using simulated solar light (AM 1.5G, 100 mW/cm^2, Bunkoukeiki CEP-25BX).

3 Results

3.1 Optical properties The standard optical transmittance spectra of the corresponding PEDOT:PSS(GO) films with different GO contents coated on glass are shown in Fig. 2. The optical transmittance in the 300-450 nm regions decreased with the increase of the GO content, whereas it increased in the 450-800 nm wavelength regions [8]. Thus, there exists an appropriate GO content for the extension of the transmittance in entire wavelength region (10-25 wt%). The microscope observation of the films revealed that GO flake sheet was distributed uniformly in the composite film. These findings imply that the optical transmittance of PEDOT:PSS(GO) layer is determined by the film thickness, fine structure of PEDOT:PSS conjugated polymer as well as the partially reduced GO content in the films. The Go addition promote the reconstruction of the PEDOT:PSS fine structure including the uniaxial anisotropic optical property [9].

3.2 Dark current-voltage characterization The dark current density-voltage (J_d-V) characteristics of heterojunction devices with different GO contents are shown in Fig. 3(a). Obviously, the current densities in reverse and forward bias are lower for devices with higher GO content. It is well known that the dark current density in a junction is determined by majority carrier injection into the metal anode, so this reduction in current density can be attributed to conductive drop across the organic layer. In Fig. 3(b), dark forward/reverse J_d-V curves is shown for the 12.5 wt% GO added PEDOT:PSS device. Three distinctively different conductive regions can be confirmed. The current increased linearly with the applied voltage in low forward bias region (region I, V < 0.1 V) and exponentially with the voltage applied in the intermediate voltage region (region II, V = 0.1-0.5 V). Further the current increases more slowly and deviates from exponential behaviour in the higher voltage region (region III, V > 0.5 V). The different conductive regions indicate a corresponding change in the carrier transport mechanism.

In region I, the forward and reverse currents were almost the same and they showed a linear relationship. This indicates the presence of a parallel current path due to a shunt resistance R_{sh} parallel to the junction.

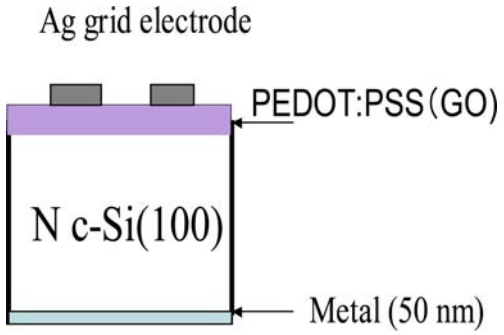

Figure 1 Schematic of the devices structure used in this study.

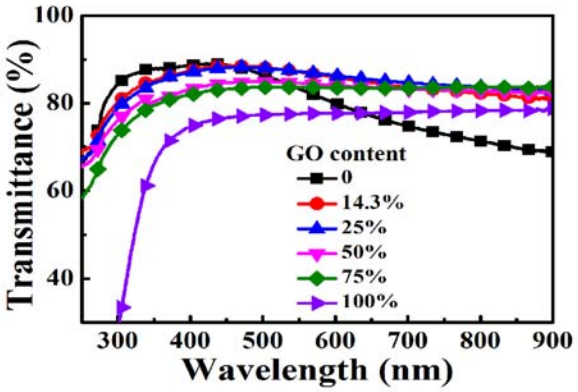

Figure 2 Optical transmittance spectra of spin-coated PEDOT:PSS(GO) composite with different GO contents on glass.

The calculated R_{sh} increased from 2.55×10^4 to 7.78×10^4 $\Omega\cdot cm^2$ with the increase of GO content, thus, enhances the insulating property. The series resistance R_s of the corresponding PEDOT:PSS:GO devices was 4.65-5 Ω, which was almost independent of GO content up to 20 wt%, and it increased up to 8.02 Ω for further increase of GO content. These results imply that the junction property is not influenced by the GO addition up to 20 wt% without creating additional defects at the junction interface.

In region II, a feature of the current is that the increase is exponential with the voltage applied, indicating that a different carrier transport mechanism dominates compared to region I. To determine the diode dominant current transport mechanisms, temperature-dependent dark current versus voltage (J_d-V-T) characteristic measured in the temperature range 293-363 K. The temperature dependence of the saturation dark current density J_0 and pre-exponential term A (= q/nkT) of the diode were extracted by fitting the *J*-V curves using a diode equation

$J(V,T)= J_o(T)[\exp(AV)-1]$ where $J_0 \propto \exp(-E_a/kT)$ (1)

where E_a is the activation energy k is the Boltzmann constant. A had a linear dependence with $1/kT$. From the temperature dependence of A, the ideality factors n = 1.12-2.91 were obtained at temperature ranging from 293 to 363 K.

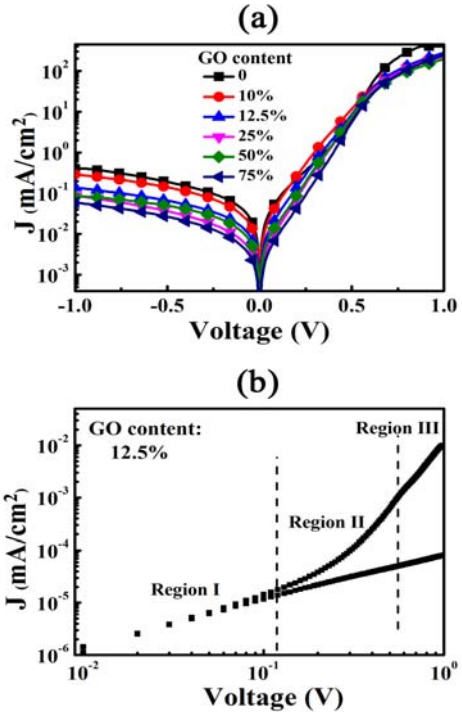

Figure 3 (a) J_d-V characteristics for c-Si/PEDOT:PSS devices with different GO contents. (b) Log J_d- log V curves for the 12.5 wt% added PEDOT:PSS device.

Furthermore, there is also a linear relationship of J_0 versus 1/kT in a semi-log representation. E_a obtained from the Arrhenius plot of J_0 decreased from 0.64 to 0.375 eV with the increase of GO content. Analyzing these results, the E_a was 0.5-0.6 eV for the GO content of 0-20 wt% and decreased to 0.375 eV with increasing GO content. Thus, the carrier transport mechanism changed from the diffusion (n = 1.0) to the space-charge recombination (n < 2) with the increase of GO content. These finings originated from the creation of defects owing to the rearrangement of the polymer chain. In addition, the J_d-V characteristics deviated from the ideal behavior at the forward voltage increased above 0.5 V. The current density shows a power law dependence of the form $J_d \propto V^m$ where m~2 indicating that J_d in the PEDOT:PSS(GO) layer is a space charge limited current (SCLC) dominated by a single trapping level.

3.3 Photovoltaic properties The J-V curves for the c-Si/PEDOT:PSS(GO) heterojunction photovoltaic devices with different GO contents are shown in Fig. 4(a) under illumination of AM 1.5G 100 mW/cm^2 light exposure. The QE spectra for the corresponding devices are also shown in Fig. 4(b). The device for the pristine PEDOT:PSS buffer layer gives a η of 6.62%, a J_{sc} of 21.5 mA/cm^2, a V_{oc} of 0.508 V, and a FF of 0.606. Once small amount of GO was mixed in PEDOT:PSS, η increased to 8.53% with a J_{sc} of 27.36 mA/cm^2, a V_{oc} of 0.532 V, and a FF of 0.6 for the PEDOT:PSS cell with a GO content of 12.5 wt%. In addition, η increased to 10.72% with a J_{sc} of 28.95 mA/cm^2, a V_{oc} of 0.548 V, and a FF of 0.675 at a GO content of 12.5 wt% for the PEDOT:PSS(GO) layer thickness of 80-100 nm. Obviously, the improvement in the device performance can be attributed to the usage of the PEDOT:PSS(GO) composite. The quantum efficiency (QE) of a solar cell permits an examination of how

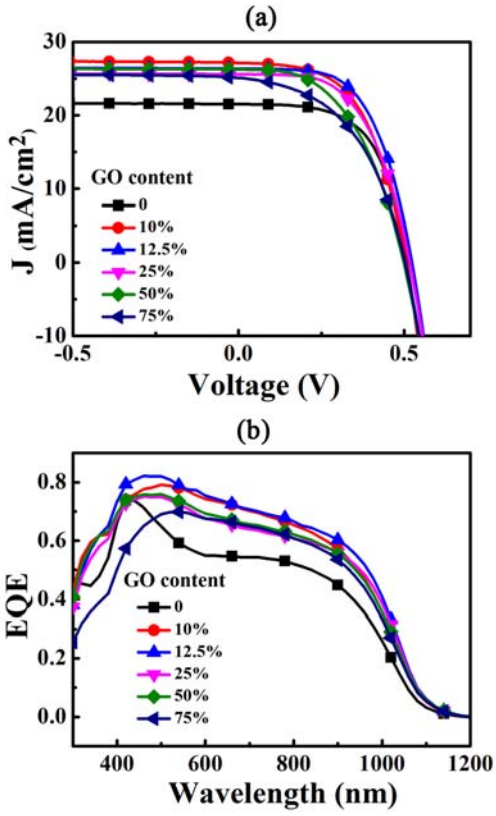

Figure 4 (a) The J-V characteristics of c-Si/PEDOT:PSS(GO) heterojunction devices under AM1.5G 100 mW/cm^2 white light illumination. (b) QE spectra of the corresponding solar cells.

photons of different wavelengths contribute to the short-circuit current. The QE improved markedly in the visible and near-infrared region for the PEDOT:PSS(GO) composite devices compared to those of pristine PEDOT:PSS [Fig. 4(b)]. These findings suggest an improved charge collection ability of the buffer layer, although the QE at 300-450 nm region reduced significantly at GO content above 50%. Thus, there exists an appropriate GO content for improving QE in the wide wavelength region. The high optical transmittance over 80-90% is still maintained in the

350-900 nm region for the 12.5 wt% GO-mixed PEDOT:PSS device. This indicates that absorbed high-energy photons are not collected at the surface of the corresponding solar cell. On the other hand, the QE increased prominently in the visible-infrared region for the GO added PEDOT:PSS films. These features are consistent with those of optical transmittance.

3.4 Carrier transport mechanism of the c-Si/PEDOT:PSS:GO junction solar cells

Figure 5 shows the schematic of the band diagram of c-Si/PEDOT:PSS(GO) composite junction under small forward bias condition. The dashed lines present the dark current, or equivalently the current due to recombination. The bold lines show the photogenerated current. The bold lines show the photogenerated current. The experimental results above are summarized as follows. 1. The optical transmittance in the UV region decreased markedly, whereas it was enhanced in the visible-infrared region for the GO contents of above 20 wt%. 2. The carrier transport mechanism changed from the diffusion to the space-charge recombination with the increase of GO content. 3. The resistivity in the PEDOT:PSS(GO) increased by the GO addition. From these results, a possible mechanism of the carrier transport in c-Si/organic interface is considered as follows. In general, the solar cell performance is determined by the following three items, that is the enhanced optical transmission, the suppression of the recombination of dark electron and photogenerated hole at the anode, the enhanced internal electric field at the interface, and the improved hole transport of organic. From the results and discussion above, the most possible mechanism is attributed to the enhanced optical transmittance in the visible-infrared regions. The spectroscopic ellipsometry study also revealed that the film thickness decreased with increasing GO content. In addition, it is also reported that the hole transport property is improved by the GO addition to PEDOT:PSS [10]. These findings are very efficient to improve the diode performance. This is achieved by inserting PEDOT:PSS:GO with wider energy gap than 1.1 eV such that the lowest unoccupied molecular orbital (LUMO) of the organic is much higher than the conduction minimum (E_c) of Si. The hole barrier, given by the E_v-highest occupied molecular orbital (HOMO) offset is very close to valence band minimum (E_v) of the silicon. In general, the V_{oc} is determined from J_0 and J_{sc} through the relation: $V_{oc}= nkT/q\ln(J_{sc}/J_0)$. Thus, large LUMO-$E_c$ offset result in a lower saturation dark current density and hence a larger V_{oc}. These contributions suppress the recombination efficiency of electrons and holes near the c-Si/PEDOT:PSS/Ag interface (Fig. 5). Here, the carrier transport property is mainly determined by the fine structure of host PEDOT:PSS polymer because the guest GO content is as low as 10-15 wt%. As the result, the charge transfer efficiency could be enhanced due to the larger drift driving force, leading to an improved J_{sc} and V_{oc}. They promote the hole collecting ability due to block of electron recombination at the Ag metal anode.

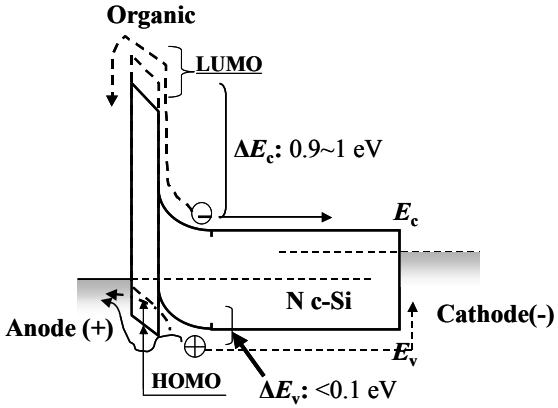

Figure 5 The band diagram of the c-Si/PEDOT:PSS(GO) composite junction under small forward bias. The dashed and bold lines represent the dark and photogenerated electron and hole currents, respectively.

4 Conclusions The optical and carrier transport properties of spin-coated PEDOT:PSS(GO) composite junction devices was studied. The GO addition into PEDOT:PSS increased the optical transmittance in the visible-infrared region and the film resistivity. The enhanced electric field at the c-Si/PEDOT:PSS(GO) interface suppressed the electron recombination at the anode. These findings imply that PEDOT:PSS(GO) composite is a possible material as a hole-collecting transparent conductive layer.

References

[1] M. Taguchi, Y. Tsunomura, H. Inoue, S. Taira, T. Nakashima, T. Baba, H. Sakata, and E. Maruyama, Proc. 24th European Photovoltaic Solar Energy Conf. 2009, p. 1690.
[2] Y. Tsunomura, Y. Yoshimine, M. Taguchi, T. Baba, T. Kinoshita, H. Kanno, H. Sakata, E. Maruyama, and M. Tanaka, Sol. Energy Mater. Sol. Cells **96**, 032105 (2010).
[3] M. Kaltenbrunner, M. S. White, E. Glowacki, T. Sekitani, R. Someya, N. S. Sariciftci, and S. Bauer, Nature Commun.; DOI.10.1038ncomms 1772 (2012).
[4] E.-G. Kim and J.-L. Bredas, J. Am. Chem. Soc. **130**, 16880 (2008).
[5] Q. Liu, Z. Tang, R. Ishikawa, K. Ueno, and H. Shirai, Appl. Phys. Lett. **100**, 183901 (2012).
[6] J. William, S. Hummers, and R. E. Offeman, J. Am. Chem. Soc. **80**, 1339 (1958).
[7] M. Hirata, T. Gotou, S. Horiuchi, M. Fujiwara, and N. Ohba, Carbon **42**, 2929 (2004).
[8] G. Eda, Y.-Y. Lin, C. Mattevi, H. Yamaguchi, H.-A. Chen, I.-S. Chen, C.-W. Chen, and M. Chhowalla, Adv. Mater. **22** 505 (2010).
[9] K. A. A. Pettersson, F. Carlsson, O. Ingenäs, and H. Arwin, Thin Solid Films **313/314**, 356 (1998).
[10] B. Yin, Q. Liu, L. Yang, X. Wu, Z. Liu, Y. Hua, S. Yin, and Y. Che, J. Nanosci. Nanotechnol. **10**, 1934 (2010).

